

## The Hydrolysis of Azetidinylium Salts. Part 2. Substituent Effects, Buffer Catalysis, and the Reaction Mechanism

Michael I. Page\* and Philip S. Webster

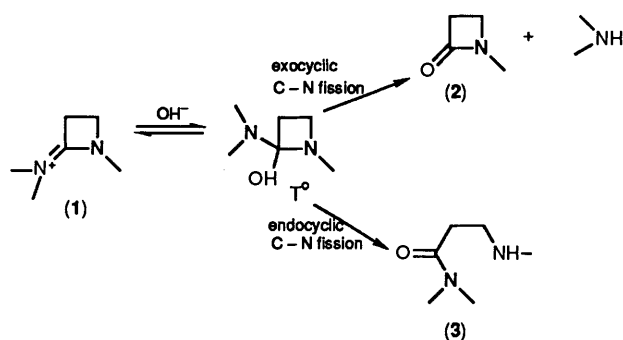
Department of Chemical Sciences, Huddersfield Polytechnic, Huddersfield HD1 3DH

Leon Ghosez

Laboratoire de Chimie Organique de Synthèse, Université Catholique de Louvain, B-1348 Louvain-La Neuve, Belgium

The hydrolysis of azetidinylium salts gives a mixture of  $\beta$ -lactams, by exocyclic C–N bond fission, and  $\beta$ -amino amides, by endocyclic C–N bond breakage and opening of the four-membered ring. The reaction is general-base catalysed and more  $\beta$ -lactam is formed using a less basic buffer. The mechanism of the buffer-catalysed reaction is the general-acid-catalysed breakdown of a reversibly formed neutral tetrahedral intermediate. The Brønsted  $\alpha$ -values vary with substituents in the amidinium salt so that they decrease with increasing electron withdrawal in the nitrogen amine which is expelled. Electron-withdrawing substituents attached to either nitrogen of the amidinium salt favour expulsion of that leaving-group amine. The Brønsted  $\beta_{1g}$  for endocyclic C–N bond fission and  $\beta$ -amino amide formation is  $-0.52$  whereas that for exocyclic C–N bond fission and  $\beta$ -lactam formation is  $-0.83$ . Substituent effects on the nitrogen amine which is not expelled but forms the product amide or  $\beta$ -lactam generate  $\beta_p$  values of  $-0.71$  and  $-0.07$ , respectively. Changes in structure–reactivity relationships with substituents are examined by an analysis of the reaction mechanism.

In the preceding paper<sup>1</sup> was reported a kinetic and product analysis study of the base-catalysed hydrolysis of azetidinylium salts (1). The reaction was shown to proceed by the formation of a neutral tetrahedral intermediate T<sup>o</sup>, which can undergo either exocyclic C–N bond cleavage to give the  $\beta$ -lactam (2) and an amine as products or endocyclic C–N bond cleavage to give the  $\beta$ -amino amide (3) (Scheme 1). Remarkably,

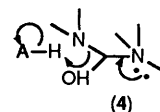


Scheme 1.

the partitioning of the intermediate is not affected by the expected release of strain energy in opening the four-membered ring and the  $\beta$ -lactam is, in fact, usually the major product.

For hydroxide-ion-catalysed hydrolysis, the breakdown of the tetrahedral intermediate occurs by water acting as a proton donor to the nitrogen in T<sup>o</sup> undergoing C–N bond cleavage (4) (HA = H<sub>2</sub>O). Herein we investigate the effect of buffer catalysis and how the partitioning of T<sup>o</sup> is affected by the acidity of the proton donor HA (4).

Substituents on both exocyclic and endocyclic nitrogens were also varied to examine their effect on the ratio of  $\beta$ -lactam to  $\beta$ -amino amide formed from the hydrolysis of azetidinylium salts (1). The partitioning of the neutral tetrahedral intermediate T<sup>o</sup> to products is expected to be influenced by



opposing factors. Electron-releasing substituents should increase the nitrogen basicity which may favour C–N bond cleavage since protonation of the nitrogen undergoing bond cleavage must occur. On the other hand, electron-withdrawing substituents should increase the nucleofugacity of the amine expelled from T<sup>o</sup>. Finally, electron-releasing substituents on the nitrogen about to become the product amide or  $\beta$ -lactam may be expected to produce a degree of electron push to facilitate C–N cleavage (4).

### Experimental

**Synthesis.**—The amidinium salts were prepared by the addition of  $\alpha$ -chloroamines to imines in dry methylene chloride at room temperature. Details of this method have been reported elsewhere,<sup>2</sup> but analytical data for the perchlorate salts are given below.

3,3-Dimethyl-1,4-diphenyl-2-(pyrrolidinium-1-ylidene)azetidinium perchlorate (5; X = H).  $\delta$ [(CD<sub>3</sub>)<sub>2</sub>SO] 7.65 (m, 10 H, 2  $\times$  Ph), 5.75 (s, 1 H, 4-H), 3.55 (m, 4 H, 2  $\times$  CH<sub>2</sub>N<sup>+</sup>), 1.90 (m, 2  $\times$  CH<sub>2</sub>), 1.60 (s, 3 H, Me), and 1.20 (s, 3 H, Me);  $\nu_{\max}$ (CH<sub>2</sub>Cl<sub>2</sub>) 1 690 (C=N<sup>+</sup>) and 1 095 cm<sup>-1</sup>.

3,3-Dimethyl-4-phenyl-2-(pyrrolidinium-1-ylidene)-1-(4-nitrophenyl)azetidinium perchlorate (5; X = OMe).  $\delta$ (CDCl<sub>3</sub>) 7.70 (d, 2 H, *o*-ArH), 7.23 (m, 5 H, Ph), 6.84 (d, 2 H, *m*-ArH), 5.28 (s, 1 H, 4-H), 3.70 (s, 3 H, OMe), 3.56 (m, 4 H, 2  $\times$  CH<sub>2</sub>N<sup>+</sup>), 2.05 (m, 4 H, 2  $\times$  CH<sub>2</sub>), 1.81 (s, 3 H, Me), and 1.20 (s, 3 H, Me);  $\nu_{\max}$ (CH<sub>2</sub>Cl<sub>2</sub>) 1 690 cm<sup>-1</sup> (C=N<sup>+</sup>).

3,3-Dimethyl-2-(morpholin-4-ium-4-ylidene)-1-(4-methoxyphenyl)-3-phenylazetidinium perchlorate.  $\delta$ (CDCl<sub>3</sub>) 8.32 (d, 2 H, *m*-ArH), 7.85 (d, 2 H, *o*-ArH), 7.30 (m, 5 H, Ph), 5.55 (s, 1 H, 4-H), 3.72 (m, 4 H, 2  $\times$  CH<sub>2</sub>N<sup>+</sup>), 1.60 (m, 4 H, 2  $\times$  CH<sub>2</sub>),

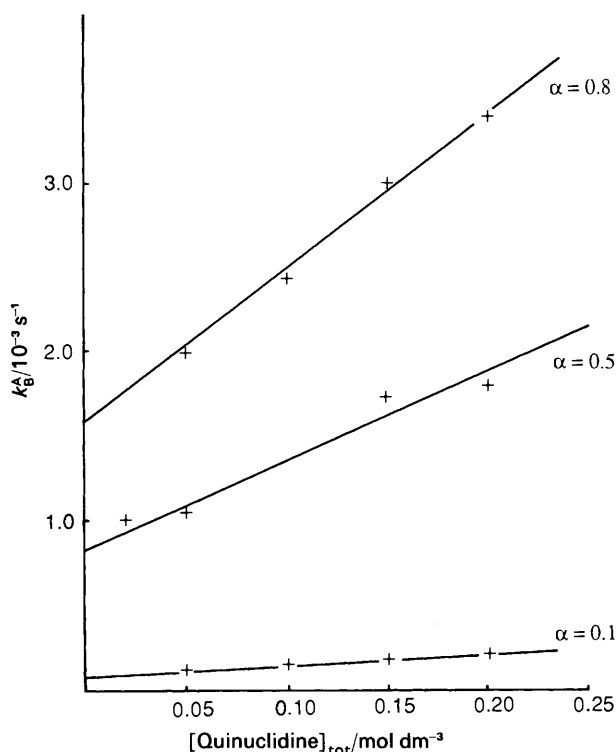
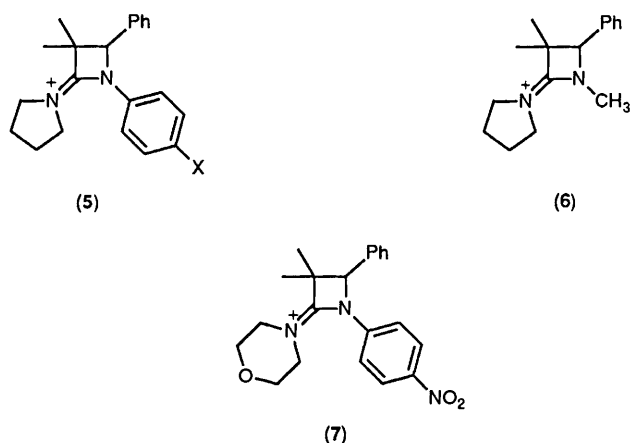


**Figure 1.** A plot of the pseudo-first-order rate constant for  $\beta$ -amino amide formation from the hydrolysis of the 4-nitrophenyl derivative (**5**; X = NO<sub>2</sub>) against the total concentration of quinuclidine buffer at 30 °C and at the fraction of free base ( $\alpha$ ) indicated.

1.85 (s, 3 H, Me), and 1.20 (s, 3 H, Me);  $\nu_{\max}(\text{CH}_2\text{Cl}_2)$  1 701  $\text{cm}^{-1}$  (C=N<sup>+</sup>).

**Product Isolation and Characterisation.**—This was carried out as described in the preceding paper.<sup>1</sup>

The products from the hydrolysis of (**5**; X = H) were separated chromatographically on silica using 9:1 (v/v) methylene chloride–ethyl acetate as the eluant: the  $\beta$ -lactam  $R_f$  0.77; the  $\beta$ -amino amide  $R_f$  0.46. The  $\beta$ -lactam from (**5**; X = H) showed  $\nu_{\max}(\text{CH}_2\text{Cl}_2)$  1 750  $\text{cm}^{-1}$  (C=O);  $\delta(\text{CDCl}_3)$  7.03 (m, 10 H, 2  $\times$  Ph), 4.81 (s, 1 H, H4), 1.49 (s, 3 H, Me), and 0.83 (s, 3 H, Me). The  $\beta$ -amino amide from (**5**; X = H) showed  $\nu_{\max}(\text{CH}_2\text{Cl}_2)$  3 370 (NH) and 1 603  $\text{cm}^{-1}$  (C=O);  $\delta(\text{CDCl}_3)$  7.26 (m, 5 H, Ph), 6.75 (m, 5 H, Ph), 5.53 (s, 1 H, NH), 4.30 (m, 1 H, H3), 3.17 (m, 4 H, 2  $\times$  CH<sub>2</sub>N), 1.63 (m, 4 H, 2  $\times$  CH<sub>2</sub>), 1.46 (s, 3 H, Me), and 1.33 (s, 3 H, Me).

The products from the hydrolysis of (**5**; X = OMe) were

eluted with 10:1 (v/v) methylene chloride–ethyl acetate: the  $\beta$ -lactam  $R_f$  0.46; the  $\beta$ -amino amide  $R_f$  0.25. The  $\beta$ -lactam from (**5**; X = OMe) showed  $\nu_{\max}(\text{CH}_2\text{Cl}_2)$  1 740 (C=O) and 1 510  $\text{cm}^{-1}$ ;  $\delta(\text{CDCl}_3)$  7.12 (m, 9 H, Ph, Ar), 4.81 (s, 1 H, 4-H), 3.83 (s, 3 H, OMe), 1.56 (s, 3 H, Me), and 0.82 (s, 3 H, Me). The  $\beta$ -amino amide from (**5**; X = OMe) showed  $\nu_{\max}(\text{CH}_2\text{Cl}_2)$  3 370 (NH) and 1 605  $\text{cm}^{-1}$  (C=O), 1 515;  $\delta(\text{CDCl}_3)$  7.13 (s, 5 H, Ph), 6.39 (dd, 4 H, Ar), 5.16 (s, 1 H, NH), 4.20 (s, 1 H, H3), 3.56 (s, 3 H, OMe), 3.16 (m, 4 H, 2  $\times$  CH<sub>2</sub>N), 1.59 (m, 4 H, 2  $\times$  CH<sub>2</sub>), 1.42 (s, 3 H, Me), and 1.26 (s, 3 H, Me).

The products from (**7**) were separated chromatographically on silica plates using 25:1 (v/v) methylene chloride–methanol as the eluant:  $\beta$ -lactam  $R_f$  0.60;  $\beta$ -amino amide  $R_f$  0.35. The  $\beta$ -lactam from (**7**) showed  $\nu_{\max}(\text{CH}_2\text{Cl}_2)$  1 760  $\text{cm}^{-1}$  (C=O);  $\delta(\text{CDCl}_3)$  8.16 (d, 2 H, ArNO<sub>2</sub>), 7.34 (m, 7 H, Ph, ArNO<sub>2</sub>), 4.93 (s, 1 H, H4), 1.56 (s, 3 H, Me), and 0.90 (s, 3 H, Me). The  $\beta$ -amino amide from (**7**) showed  $\nu_{\max}(\text{CH}_2\text{Cl}_2)$  3 410 (NH) and 1 610  $\text{cm}^{-1}$  (C=O);  $\delta(\text{CDCl}_3)$  7.92 (d, 2 H, *m*-Ar), 7.01 (s, 5 H, Ph), 6.65 (d, 2 H, *o*-Ar), 4.60 (d, 1 H, 3-H), 3.82 (m, 4 H, 2  $\times$  CH<sub>2</sub>N), 1.73 (m, 4 H, 2  $\times$  CH<sub>2</sub>), 1.75 (s, 3 H, Me), and 1.60 (s, 3 H, Me).

**HPLC of Reactants and Products.**—This was carried out as described in the preceding paper.<sup>1</sup> The retention times of reactants and products under these conditions were (**5**; X = H) 50:50 CH<sub>3</sub>CN–0.02 mol dm<sup>-3</sup> acetic acid, 3  $\times$  10<sup>-3</sup> mol dm<sup>-3</sup> tetrabutylammonium hydroxide in water, 6.7 min;  $\beta$ -amino amide, 20.0 min;  $\beta$ -lactam 17.0 min. (**5**; X = OMe) 50:50 CH<sub>3</sub>CN–0.02 mol dm<sup>-3</sup> acetic acid, 3  $\times$  10<sup>-3</sup> mol dm<sup>-3</sup> tetrabutylammonium hydroxide in water, 7.1 min;  $\beta$ -amino amide, 18.1 min;  $\beta$ -lactam, 15.1 min. (**7**) 50:50 CH<sub>3</sub>CN–0.02 mol dm<sup>-3</sup> acetic acid, 3  $\times$  10<sup>-3</sup> mol dm<sup>-3</sup> tetrabutylammonium hydroxide in water, 15.5 min;  $\beta$ -amino amide, 9.0 min;  $\beta$ -lactam, 21.3 min.

**Kinetics.**—The kinetics of the hydrolysis reactions were performed as described in the preceding paper.<sup>1</sup>

## Results and Discussion

The azetidinium amidinium salts which were studied are given by structures (**5**)–(**7**). The ratio of  $\beta$ -lactam to  $\beta$ -amino amide formed from the hydrolysis of the azetidinium amidinium salts is a complex function of pH, buffer, and nitrogen substituents. The ratio changes with pH because, as reported in the preceding paper,<sup>1</sup> there are two changes in the rate-limiting step with increasing pH. The ratio changes with the nature of the buffer because the rates of formation of the two products have different dependences upon the  $\text{p}K_a$  of the buffer catalyst. Electron-withdrawing substituents in aniline leaving groups (**5**) decrease the amount of  $\beta$ -lactam formed and thus favour endocyclic over exocyclic C–N bond fission.

It is not easy to predict the effect of substituents on the partitioning of the tetrahedral intermediate, T<sup>o</sup> (Scheme 1), because of the opposite requirements of protonation and C–N bond cleavage. As a result of this, for example, the rates of alkaline hydrolysis of amides show only a small dependence on amine substituents.<sup>3</sup> The effect of the nitrogen not undergoing C–N bond cleavage is expected to be dependent on the degree of amide/ $\beta$ -lactam resonance developed in the transition-state structure. The combination of substituent effects and Brønsted relationships have allowed the elucidation of transition state structures and a separation of the importance of these various factors.

**Buffer Catalysis.**—The hydrolysis of the substituted *N*-arylazetidinium amidinium salts is buffer catalysed. At constant pH the observed pseudo-first-order rate constants for hydro-

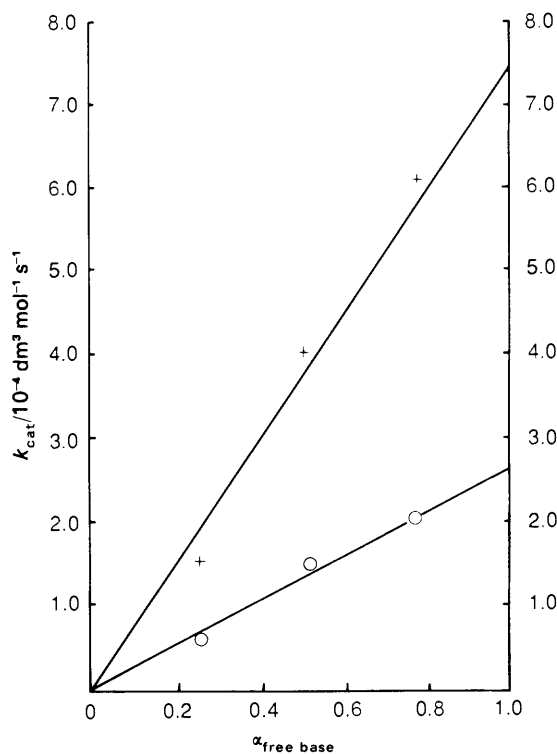
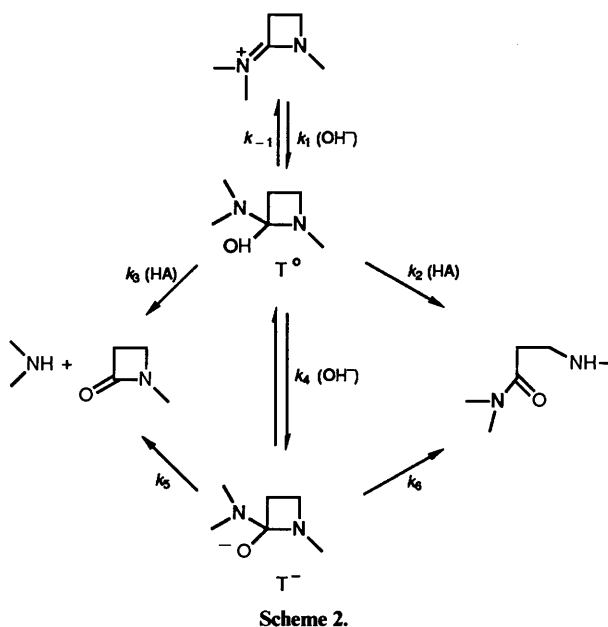


**Figure 2.** A plot of the catalytic constant  $k_{\text{cat}}$  for trifluoroethanol-catalysed hydrolysis of the phenyl derivative (**5**; X = H) against the fraction of free base ( $\alpha$ ) in the buffer: +,  $k_{\text{cat}}$  for  $\beta$ -lactam formation; O,  $k_{\text{cat}}$  for  $\beta$ -amino amide formation.



lysis increase linearly with increasing total buffer concentration for both  $\beta$ -lactam and  $\beta$ -amino amide formation (Figure 1). The slopes of these plots are designated  $k_{\text{cat}}^{\text{L}}$  and  $k_{\text{cat}}^{\text{A}}$  for  $\beta$ -lactam and  $\beta$ -amino amide formation, respectively. Plots of  $k_{\text{cat}}$  against  $\alpha$ , the fraction of buffer which is in its basic form, are linear and pass through the origin at  $\alpha = 0$  (Figure 2). This indicates that buffer catalysis occurs by the basic form of the buffer and that the acid form is inactive. The intercept of  $k_{\text{cat}}$  against  $\alpha$  at  $\alpha = 1$  gives the second-order rate constant for the base-catalysed

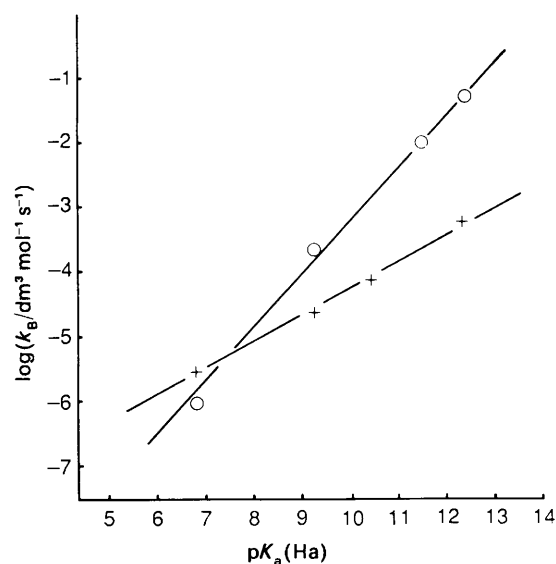


**Figure 3.** Brønsted plot for  $\beta$ -lactam (+) and  $\beta$ -amino amide formation (O) for the kinetically general-base-catalysed hydrolysis of the 4-nitrophenyl amidinium salt (**5**; X = NO<sub>2</sub>).

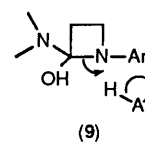
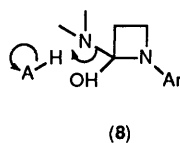
reaction. The ratio of  $\beta$ -lactam to  $\beta$ -amino amide formed is independent of the buffer concentration at constant pH. This also indicates that both reactions follow the same rate law. The only exception to this behaviour is in carbonate buffers for which  $k_{\text{cat}}$  shows a non-linear dependence upon  $\alpha$  and is described in the preceding paper.<sup>1</sup>

Kinetically the buffer dependence is apparent general-base catalysis, equation (1) where  $k_{\text{B}}^{\text{L}}$  and  $k_{\text{B}}^{\text{A}}$  are the second-order rate constants for buffer catalysed  $\beta$ -lactam and  $\beta$ -amino amide formation, respectively. However, mechanistically, this is probably the kinetically equivalent general-acid-specific-base-catalysed reaction equation (2), where  $K_{\text{a}}$  and  $K_{\text{w}}$  are the dissociation constants for the conjugate acid of the buffer BH<sup>+</sup> and water, respectively. The observed second-order rate constants for the buffer-catalysed hydrolysis of the azetidinium amidinium salts are given in Table 1.

$$k_{\text{obs}} - k_0 = k_{\text{B}}^{\text{L}}[\text{B}] + k_{\text{B}}^{\text{A}}[\text{B}] \quad (1)$$

$$k_{\text{obs}} - k_0 = \frac{k_{\text{B}}^{\text{L}} K_{\text{a}}}{K_{\text{w}}} [\text{BH}^+][\text{OH}^-] + \frac{k_{\text{B}}^{\text{A}} K_{\text{a}}}{K_{\text{w}}} [\text{BH}^+][\text{OH}^-] \quad (2)$$

The buffer-catalysed reaction therefore represents general-acid-catalysed breakdown of the reversibly formed neutral tetrahedral intermediate T<sup>0</sup>,  $k_2$  and  $k_3$  (Scheme 2). The function of the catalyst is to facilitate both exocyclic (**8**) and endocyclic (**9**) C–N bond fission.



It is interesting to note that even for the *N*-(4-nitrophenyl) derivative (**5**; X = NO<sub>2</sub>) proton donation is required to facilitate C–N bond fission despite the relatively good leaving group and the strain energy that is released upon ring opening.<sup>4</sup>

The Brønsted plots for these buffer-catalysed reactions are shown in Figure 3. For the *N*-(4-nitrophenyl) derivative (**5**; X = NO<sub>2</sub>) the slope of the line ( $\beta$ ) is 0.41 for  $\beta$ -lactam formation and

**Table 1.** The second-order rate constants ( $\text{dm}^3 \text{mol}^{-1} \text{s}^{-1}$ ) for the buffer-catalysed hydrolysis of azetidinylium salts in water at  $30^\circ\text{C}$  and  $I = 1.0 \text{ mol dm}^{-3}$  (KCl).

Buffer	$pK_a$	(5; X = NO <sub>2</sub> )		(5; X = H)		(5; X = OMe)	
		$k_B^L$	$k_B^A$	$k_B^L$	$k_B^A$	$k_B^L$	$k_B^A$
Water	15.74	$1.50 \times 10^{-2}$	$1.44 \times 10^{-1}$	$1.00 \times 10^{-2}$	$1.04 \times 10^{-3}$	$6.61 \times 10^{-3}$	$1.65 \times 10^{-3}$
Trifluoroethanol	12.43	$5.30 \times 10^{-4}$	$5.20 \times 10^{-2}$	$7.35 \times 10^{-4}$	$2.54 \times 10^{-4}$	$2.52 \times 10^{-4}$	$3.05 \times 10^{-4}$
Quinuclidine	11.55	$< 1 \times 10^{-4}$	$1.08 \times 10^{-2}$	$2.30 \times 10^{-4}$	$1.26 \times 10^{-4}$	$1.40 \times 10^{-4}$	$1.50 \times 10^{-4}$
Carbonate	10.30	$8.00 \times 10^{-5}$	$< 5 \times 10^{-5c}$	$1.50 \times 10^{-5}$	$< 5 \times 10^{-6d}$		
1,1,1,3,3,3-Hexafluoro- propan-2-ol	9.30	$2.17 \times 10^{-5}$	$2.36 \times 10^{-4}$	$1.16 \times 10^{-5}$	$3.98 \times 10^{-6}$		
Phosphate	6.80	$2.90 \times 10^{-6}$	$9.96 \times 10^{-7}$	$5.62 \times 10^{-7}$	$1.78 \times 10^{-7}$		
Acetate	4.70	$1.43 \times 10^{-6}$	$1.36 \times 10^{-6}$				
		(6) <sup>a</sup>		(7)			
Buffer		$k_B^L$	$k_B^A$	$k_B^L$	$k_B^A$		
Water		$6.49 \times 10^{-4}$	$5.03 \times 10^{-4}$	3.80	16.3		
Trifluoroethanol		$2.52 \times 10^{-4}$	$3.05 \times 10^{-4}$	$2.05 \times 10^{-1}$	1.60		
Quinuclidine		$1.40 \times 10^{-4}$	$1.50 \times 10^{-4}$	$9.44 \times 10^{-2}$	$1.94 \times 10^{-1}$		
Carbonate							
1,1,1,3,3,3-Hexafluoro- propan-2-ol		$6.32 \times 10^{-6}$	$3.16 \times 10^{-6}$	$3.30 \times 10^{-3}$	$9.80 \times 10^{-3}$		
Phosphate				$4.96 \times 10^{-5}$	0.28 <sup>b</sup>		
Acetate							

<sup>a</sup> Rate constants for propylamine and ethylenediamine are  $k_B^L 6.31 \times 10^{-5}$  and  $2.14 \times 10^{-5} \text{ dm}^3 \text{mol}^{-1} \text{s}^{-1}$ , respectively;  $k_B^A = 5.01 \times 10^{-5}$  and  $7.08 \times 10^{-6} \text{ dm}^3 \text{mol}^{-1} \text{s}^{-1}$ , respectively. <sup>b</sup> Value for phosphate trianion, see the text. <sup>c</sup>  $k_B^L[\text{OH}^-][\text{CO}_3^{2-}]$  is  $6.02 \times 10^{-1} \text{ dm}^6 \text{mol}^{-2} \text{s}^{-1}$ . <sup>d</sup>  $k_B^L[\text{OH}^-][\text{CO}_3^{2-}]$  is  $2.65 \times 10^{-3} \text{ dm}^6 \text{mol}^{-2} \text{s}^{-1}$ .

**Table 2.** Second- and third-order rate constants for the hydroxide-ion-catalysed hydrolysis of azetidinylium salts in water at  $30^\circ\text{C}$  and  $I = 1.0 \text{ mol dm}^{-3}$  (KCl).<sup>a</sup>

Amidinium salt	$k_{\text{OH}^-}^L/\text{dm}^3 \text{mol}^{-1} \text{s}^{-1}$	$k_{\text{OH}^-}^A/\text{dm}^3 \text{mol}^{-1} \text{s}^{-1}$	$k_{\text{OH}^-}^A/\text{dm}^3 \text{mol}^{-1} \text{s}^{-1}$	$k_{\text{OH}^-}^A/\text{dm}^6 \text{mol}^{-2} \text{s}^{-1}$
(5; X = NO <sub>2</sub> )	$1.50 \times 10^{-2}$	$1.44 \times 10^{-1}$	$4.10 \times 10^{-1}$	73.2
(5; X = H)	$1.00 \times 10^{-2}$	$1.04 \times 10^{-3}$	$2.60 \times 10^{-3}$	$3.02 \times 10^{-1}$
(5; X = OMe)	$6.61 \times 10^{-3}$	$1.65 \times 10^{-3}$	$9.40 \times 10^{-4}$	$9.22 \times 10^{-2}$
(6)	$6.49 \times 10^{-4}$	$5.03 \times 10^{-4}$	$7.06 \times 10^{-3}$	$2.54 \times 10^{-3}$
(7)	3.80	16.3		

<sup>a</sup> The rate constants are defined in equation (5).

0.83 for  $\beta$ -amino amide formation. More  $\beta$ -lactam is formed using a less basic buffer. These Brønsted  $\beta$ -values are equivalent to  $\alpha$ -values of 0.59 and 0.17, respectively, for  $\beta$ -lactam and  $\beta$ -amino amide formation in the general-acid-catalysed pathway. The higher  $\alpha$  value for  $\beta$ -lactam formation indicates that exocyclic C–N bond cleavage is more dependent than endocyclic ring opening upon the acidity of the proton donor. This is perhaps not surprising in view of the large difference in basicity between the exocyclic and endocyclic nitrogens in the neutral tetrahedral intermediate T<sup>o</sup> (8).

The Brønsted  $\alpha$ -values for  $\beta$ -lactam and  $\beta$ -amino amide formation from the *N*-phenylazetidinylium salt (5; X = H) are 0.43 and 0.40, respectively. The decrease in  $\alpha$  from 0.40 to 0.17 for  $\beta$ -amino amide formation and opening the four-membered ring occurs as the substituent in the aromatic ring is made more electron withdrawing *i.e.* as the nitrogen becomes less basic. The  $\alpha$  value for exocyclic bond fission and  $\beta$ -lactam formation increases from 0.43 to 0.59 on going from the phenyl to the 4-nitrophenyl derivative. It is expected that the nitro substituent will decrease the amount of electron push from the ring nitrogen in facilitating exocyclic C–N bond fission *i.e.*  $\beta$ -lactam formation becomes more dependent on the acidity of the catalyst as substituents on the ring nitrogen become more electron withdrawing.

Buffer catalysis is also observed for the hydrolysis of the *N*-alkylazetidinylium salts. For the *N*-methyl derivative (6) the Brønsted  $\beta$ -value for the general-base-catalysed  $\beta$ -lactam formation is 0.55 which is equivalent to an  $\alpha$  value of 0.45 in the proposed general-acid-catalysed mechanism.  $\beta$ -Amino amide formation from ring opening exhibits a Brønsted  $\beta$ -value of 0.68 equivalent to an  $\alpha$  value of 0.32.

The reactivity of the *N*-methyl derivative (6) is similar to that of the *N*-phenylazetidinylium salt (5; X = H). The second-order rate constants for  $\beta$ -amino amide formation are almost identical for (6) and (5; X = H) (Table 2). Although aniline may be considered a better leaving group than methylamine, based on the stability of their anions, the alkyl substituent makes the nitrogen more basic, which favours protonation. In the concerted reaction pathway both proposed basicity and leaving-group ability are important. The alkaline hydrolysis rates of acetanilide is about 40 times greater than that of *N*-methylacetamide.<sup>3</sup> For  $\beta$ -lactam formation from the amidinium salts the *N*-phenyl compound (5; X = H) is about 15 times more reactive than the *N*-methyl derivative (6) for alkaline hydrolysis but only about twice for buffer-catalysed hydrolysis.

The effect of making the exocyclic nitrogen less basic also has an effect upon the Brønsted exponents. The morpholine derivative (7) has a nitrogen 3  $pK_a$  units less basic than the pyrrolidine compounds (5). The hydrolysis of (7) is buffer catalysed and, with the exception of phosphate buffers, the ratio of  $\beta$ -lactam to  $\beta$ -amino amide formed is independent of buffer concentration. The Brønsted  $\beta$  value for  $\beta$ -lactam formation is 0.64 which is equivalent to an  $\alpha$  value of 0.36 for the general-acid-catalysed mechanism. The  $\alpha$  value for  $\beta$ -lactam formation from (5; X = NO<sub>2</sub>) is 0.59, so again the  $\alpha$  value is reduced by having a better leaving group in the sense of a more weakly basic amine, the morpholine leaving group requiring less protonation than the more basic pyrrolidine. This is similar to the observation for endocyclic C–N bond fission. The buffer-catalysed formation of a  $\beta$ -amino amide from the morpholino derivative (7) exhibits an observed Brønsted  $\beta$  value of 0.75, equivalent to a calculated  $\alpha$  value of 0.25 for general-acid-catalysed breakdown of the

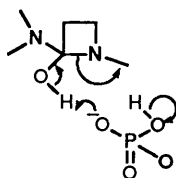
**Table 3.** Brønsted exponents  $\alpha$  for the general-acid-catalysed breakdown of the tetrahedral intermediate T<sup>o</sup> formed from the hydrolysis of azetidiny amidinium salts (Scheme 2).

Brønsted exponent	Amidinium salt			
	(5; X = NO <sub>2</sub> )	(5; X = H)	(6)	(7)
$\alpha$ (Amino amide)	0.17	0.40	0.32	0.25
$\alpha$ ( $\beta$ -Lactam)	0.59	0.43	0.45	0.36

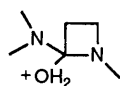
**Table 4.** Observed and calculated microscopic rate and equilibrium constants for the hydrolysis of azetidiny amidinium salts. The constants are defined in Scheme 2.

	$k_1/\text{dm}^3 \text{ mol}^{-1} \text{ s}^{-1}$	$k_{-1}/\text{s}^{-1}$	$K_2/\text{dm}^3 \text{ mol}^{-1}$	$k_2/\text{s}^{-1}$
(5; X = NO <sub>2</sub> )	$4.10 \times 10^{-1}$	$5.61 \times 10^7$	$7.32 \times 10^{-9}$	$1.97 \times 10^7$
(5; X = H)	$2.60 \times 10^{-3}$	$8.62 \times 10^7$	$3.02 \times 10^{-11}$	$3.44 \times 10^7$
(5; X = OMe)	$9.40 \times 10^{-4}$	$1.02 \times 10^8$	$9.22 \times 10^{-12}$	$1.79 \times 10^8$
(6)	<i>a</i>	$2.54 \times 10^{-3}$	$3.60 \times 10^9$	$7.06 \times 10^{-13}$
	<i>b</i>	$1.69 \times 10^{-3}$	$2.20 \times 10^9$	$7.68 \times 10^{-13}$

<sup>a</sup> From amino amide formation. <sup>b</sup> From  $\beta$ -lactam formation.



(10)



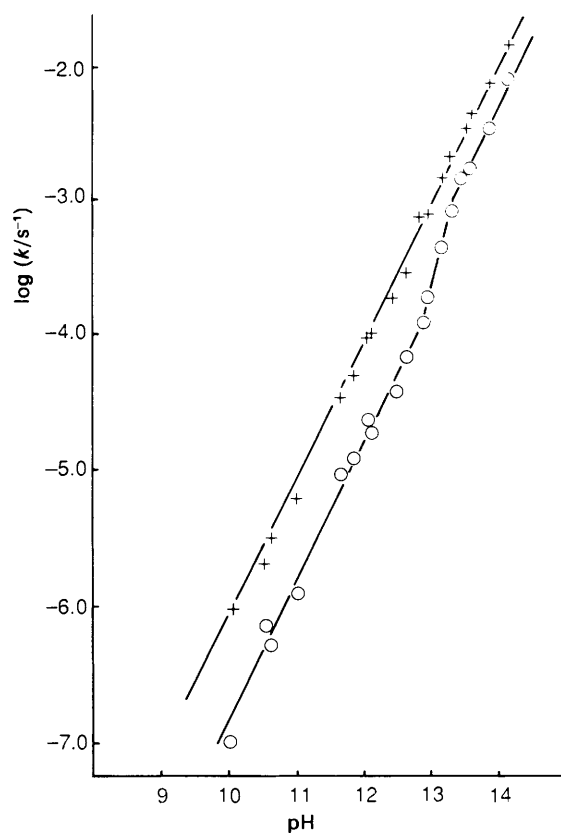
(11)

tetrahedral intermediate. This  $\alpha$  value may be compared with that of 0.17 for (5; X = NO<sub>2</sub>). In this case the reduced electron push provided by the remaining nitrogen, morpholine *versus* pyrrolidine, has little effect upon the degree of protonation of the leaving group, 4-nitroaniline, although  $\alpha$  is slightly increased. The Brønsted  $\alpha$  values for the buffer-catalysed hydrolysis are summarised in Table 3.

The phosphate-catalysed hydrolysis of 7 to give a  $\beta$ -amino amide shows a term in the rate law which is first order in hydroxide ion and hydrogenphosphate dianion [equation (3)].

$$k_{\text{obs}} - k_0 = k_{\text{B}}^{\text{L}}(\text{HPO}_4^{2-}) + k_{\text{B}}^{\text{A}}(\text{HPO}_4^{2-})(\text{OH}^-) \quad (3)$$

As  $\beta$ -lactam and  $\beta$ -amino amide formation have different kinetic dependences the proportion of  $\beta$ -lactam produced increases with decreasing pH. Although the third-order term for  $\beta$ -amino amide formation is reminiscent of the carbonate-hydroxide term observed for the *N*-pyrrolidine derivative,<sup>1</sup> hydrogenphosphate dianion can act as both a proton donor and acceptor. By analogy with the bifunctional catalysis proposed for imidate ester hydrolysis<sup>5</sup> it might be assumed that this occurs in the breakdown of the neutral tetrahedral intermediate (10). However the third-order term is kinetically equivalent to phosphate trianion catalysis [equation (4)], where  $K_{\text{w}}$  and  $K_{\text{a}}$  are the dissociation constants for water and monohydrogenphosphate dianion, respectively. The calculated second-order

**Figure 4.** The pH-rate profile for the hydrolysis of the *N*-phenyl derivative (5; X = H) at 30 °C:  $k$  = the pseudo-first-order rate constant for  $\beta$ -lactam (+) and  $\beta$ -amino amide (O) formation.

$$k_{\text{B}}^{\text{A}}(\text{HPO}_4^{2-})(\text{OH}^-) = k_{\text{B}}^{\text{L}} \frac{K_{\text{w}}}{K_{\text{a}}} (\text{PO}_4^{3-}) \quad (4)$$

rate constant for phosphate trianion catalysis is  $0.28 \text{ dm}^3 \text{ mol}^{-1} \text{ s}^{-1}$  which, in fact, fits the Brønsted plot for the general-base-catalysed hydrolysis of (7) to the corresponding  $\beta$ -amino amide. There is thus no evidence for any bifunctional catalysis by phosphate buffers.

The general conclusion about buffer-catalysed hydrolysis of the azetidiny amidinium salts is that both  $\beta$ -amino amide and  $\beta$ -lactam formation show a dependence on the basicity of the buffer which in turn shows a degree of sensitivity to substituent effects. These will be discussed in greater detail in the section on the mechanism of hydrolysis.

Below pH 6.5, the rate of hydrolysis of the amidinium compound (5; X = NO<sub>2</sub>) becomes pH independent and faster than the calculated rate of formation of T<sup>o</sup> by the addition of hydroxide ion ( $k_1[\text{OH}^-]$ ; Scheme 2).<sup>1</sup> The mechanism of hydrolysis at low pH must therefore involve initial attack by water on the amidinium compound. The observed buffer catalysis by acetate could be due to either general-base-catalysed addition of water or deprotonation/protonation of the tetrahedral intermediate (11).

*Substituent Effects on Alkaline Hydrolysis.*—(a) *Endocyclic nitrogen.* The ratio of  $\beta$ -lactam to  $\beta$ -amino amide formed from the hydrolysis of the *N*-aryl substituted derivatives (5) changes with pH as is shown in Figure 4 for the *N*-phenyl derivative. This is because at pH > 12 the rate of  $\beta$ -amino amide formation shows a second-order dependence upon hydroxide ion which at even higher pH reverts to a first-order dependence. In the previous paper<sup>1</sup> it is shown that this is due to the conversion by hydroxide ion, of the neutral tetrahedral intermediate into its

anion which only decomposes to the  $\beta$ -amino amide. Throughout the pH region investigated the rate of  $\beta$ -lactam formation remains first order in hydroxide ion. The experimental second- and third-order rate constants are given in Table 2 and are defined by equation (5), where  $k_{\text{obs}}$  is the observed pseudo-first-

$$k_{\text{obs}} = k_{\text{OH}}^{\text{L}}[\text{OH}^-] + k_{\text{OH}}^{\text{A}}[\text{OH}^-] + \frac{k_{\text{OH}}^{\text{A}} k_{\text{OH}'}^{\text{A}} [\text{OH}^-]^2}{k_{\text{OH}'}^{\text{A}} + k_{\text{OH}}^{\text{A}} [\text{OH}^-]} \quad (5)$$

order rate constant, the superscripts L and A refer to  $\beta$ -lactam and  $\beta$ -amino amide formation, respectively. The subscripts OH and OH' refer to the second-order rate constants for product formation at low and high pH, respectively. The subscript OH'' refers to the third-order rate constant which is second order in hydroxide ion.

The effect of aryl substituents on the second-order rate constants  $k^{\text{L}}$  and  $k^{\text{A}}$  may be correlated by a Brønsted relationship by plotting the logarithm of the rate constant against the  $\text{p}K_{\text{a}}$  of the amine. The slope of this line defines two Brønsted exponents— $\beta_{1\text{g}}$  for  $\beta$ -amino amide formation and endocyclic C–N bond fission (9) and  $\beta_{\text{p}}$  for  $\beta$ -lactam formation which provides a measure of the electron 'push' provided for exocyclic C–N bond fission (8). The Brønsted  $\beta_{1\text{g}}$  for  $\beta$ -amino amide formation is  $-0.52$ , with electron-withdrawing substituents in the aryl ring of (5) facilitating  $\beta$ -lactam ring opening and formation of the  $\beta$ -amino amide product. It is expected that such substituents will increase the equilibrium constant for formation of the tetrahedral intermediate  $\text{T}^\circ$  (Scheme 2) but their overall effect on C–N bond fission comprises two opposing factors. Protonation of the leaving group aniline is known to occur because of the observed buffer catalysis and electron-withdrawing groups in the aromatic ring will reduce the basicity and inhibit protonation. Conversely, these electron-withdrawing substituents would stabilise the amine anion and facilitate C–N cleavage. The measured Brønsted  $\beta_{1\text{g}}$  is the sum effect of all these factors.

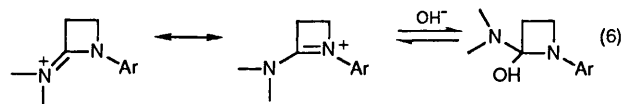
It is not possible to interpret readily the  $\beta$ -value in terms of transition structures because the effective charge<sup>6</sup> on the endocyclic nitrogen in the amidinium salt is not known. There is no evidence that resonance in four-membered rings is reduced from that in analogous acyclic systems<sup>7</sup> and it is therefore assumed that the four-membered ring nitrogen carries considerable positive charge. It is probable that the effective charge on the endocyclic nitrogen is at least  $+0.5$  and so the observed  $\beta_{1\text{g}}$  of  $-0.52$  is compatible with a transition in which this charge is largely removed. This could be due to either the transition state resembling the tetrahedral intermediate  $\text{T}^\circ$  or an approximate balance between negative-charge development on nitrogen due to C–N fission and positive charge development due to protonation (9). The Brønsted  $\alpha$  values observed for the general acid-catalysed breakdown of the tetrahedral intermediate indicate that a significant amount of proton transfer occurs in the transition state. The degree of bond making and breaking in the transition state is discussed in greater detail in the following section.

The effect of substituents in the aryl ring on the rate of exocyclic fission and  $\beta$ -lactam formation is small and the Brønsted  $\beta_{\text{p}}$  value is  $-0.07$ . Overall this indicates little change in the effective charge on the ring nitrogen on going from the initial reactant state to the transition state. It is compatible with considerable positive charge on the developing  $\beta$ -lactam nitrogen in the transition state (8) and hence with significant exocyclic C–N bond fission.

It is possible to estimate the effect of substituents on the microscopic rate constants defined in Scheme 2. The values of these constants may be deduced if it is assumed that the rate term which is second order in hydroxide ion represents rate-limiting and diffusion-controlled deprotonation of the neutral

tetrahedral intermediate  $\text{T}^\circ$  to form the anionic form  $\text{T}^-$  (Scheme 2). The observed third-order rate constant is then given by  $k_4 K_1$  and if  $k_4$  is taken to be  $10^{10} \text{ dm}^3 \text{ mol}^{-1} \text{ s}^{-1}$  the value of  $K_1$  the equilibrium constant for formation of the neutral tetrahedral intermediate  $\text{T}^\circ$ , can be calculated.<sup>1</sup> Other microscopic rate constants can be estimated as outlined in the previous paper<sup>1</sup> and the values of these are given in Table 4.

Electron-withdrawing substituents in the endocyclic aryl amine increase the calculated equilibrium constant for formation of the neutral tetrahedral intermediate  $\text{T}^\circ$  and the Brønsted  $\beta$ -value is  $-0.66$ . This is surprisingly high and may indicate, in fact, that the rate-limiting step for the term second order in hydroxide is not diffusion-controlled deprotonation of the tetrahedral intermediate but some subsequent step. Taken at its face value, however, the high Brønsted value is indicative of a large change in positive charge density on the endocyclic nitrogen upon formation of the tetrahedral intermediate. The effective charge density on the endocyclic nitrogen is not known, although resonance would suggest a share of positive charge between the endo- and exo-cyclic nitrogens [equation (6)].



However, given the disparity between the basicity of aryl and alkyl amines one would expect the greater charge to reside on the exocyclic nitrogen. If the assumption about rate-limiting deprotonation is correct, then the Brønsted  $\beta$  value of  $-0.66$  indicates that the effective charge 'felt' by the aryl substituents is about two-thirds of that in protonated anilines with significant positive charge on the endocyclic nitrogen.

As expected, electron-withdrawing substituents in the endocyclic aryl amine also increase the rate of formation of the neutral tetrahedral intermediate  $\text{T}^\circ$  and the Brønsted  $\beta$ -value for  $k_1$  is  $-0.61$ . The effect of these substituents on breakdown of  $\text{T}^\circ$  to reactants *i.e.* the reverse step  $k_{-1}$  is small and in the opposite direction generating a  $\beta$  value of  $+0.05$ . This is compatible with considerable carbon–oxygen bond formation in the transition state for formation of  $\text{T}^\circ$  from hydroxide ion attack on the amidinium carbon.

Based on the assumption of diffusion-controlled deprotonation of  $\text{T}^\circ$  by hydroxide ion the rate constants for the uncatalysed breakdown to  $\beta$ -amino amide  $k_2$  (Scheme 2) may also be calculated (Table 4), since the observed second-order rate constant for the hydroxide-ion-catalysed hydrolysis at low pH,  $k_{\text{OH}} = k_1 k_2 / (k_{-1} + k_2)$ . Electron-releasing substituents in the endocyclic arylamine increase the calculated rate of breakdown of  $\text{T}^\circ$ ,  $k_2$ , (Table 4) and generate a Brønsted  $\beta_{1\text{g}}$  of  $+0.14$ . These rate constants are too fast for rate-limiting deprotonation of  $\text{T}^\circ$  by water and, in any case, such a process would generate a negative  $\beta$  value. The rate constants are also too fast for stepwise protonation of the weakly basic aryl nitrogen by water. The results are compatible with rate-limiting general-acid-catalysed breakdown of  $\text{T}^\circ$  by water acting as a proton donor to the endocyclic nitrogen (12). This pathway



would formally generate a protonated amide as the initial product. In the previous section, buffer-catalysed  $\beta$ -amino

amide formation is interpreted as a similar general acid catalysed breakdown of  $T^\circ$ . An alternative interpretation is that  $k_2$  represents a rate-limiting proton-switch<sup>8</sup> to generate the zwitterionic intermediate (13) which subsequently breaks down to the amino amide. However, the proton switch would be expected to occur to the more basic exocyclic nitrogen which would then generate an intermediate to give the  $\beta$ -lactam as product. The rate constants for this process have been estimated<sup>8</sup> to be in the region  $10^6$ – $10^8$  s<sup>-1</sup>. Whichever process is correct, the effect of substituents indicate that the basicity of the nitrogen is important and if protonation is concerted with C–N bond fission (12), then in the transition state the former process runs ahead of the latter.

(b) *Exocyclic nitrogen.* The effect of the basicity of the exocyclic nitrogen on the alkaline hydrolysis of the azetidiny amidinium salts was also studied by comparing the reactivity of (5; X = NO<sub>2</sub>) with that of (7).

The ratio of  $\beta$ -lactam to  $\beta$ -amino amide formed from the hydrolysis of (7) is 0.23 and is constant over the pH range 8–12. This ratio may be compared with that from (5; X = NO<sub>2</sub>) for which it is 0.10, so the decreased basicity of the exocyclic nitrogen increases the amount of  $\beta$ -lactam product. The rate of  $\beta$ -lactam and  $\beta$ -amino amide formation from (7) is first order in hydroxide-ion concentration between pH 8 and 12 and there is no second-order term in hydroxide ion over this range. The second-order rate constants for (7) are given in Table 1 from which it can be seen that the one for  $\beta$ -lactam formation is 253 times greater than that for (5; X = NO<sub>2</sub>), whereas the one for  $\beta$ -amino amide formation is 113 times greater. The increased reactivity of (7) is mainly due to a more favourable equilibrium constant for formation of the tetrahedral intermediate  $T^\circ$  (Scheme 2).

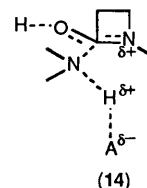
Below pH 8 the ratio of  $\beta$ -lactam to  $\beta$ -amino amide formed from the hydrolysis of (7) increases with decreasing pH. This is due to the introduction of a pH-independent 'spontaneous' hydrolysis and is also observed for the hydrolysis of (5; X = NO<sub>2</sub>).<sup>1</sup>

A comparison of the second-order rate constants for the hydroxide-ion-catalysed hydrolysis of (7) with those of (5; X = NO<sub>2</sub>) (Table 1) allows the deduction of Brønsted  $\beta$  values for the effect of the exocyclic nitrogen on exocyclic C–N bond fission and  $\beta$ -lactam formation,  $\beta_{1g}^L$ , and endocyclic C–N bond fission and  $\beta$ -amino amide formation,  $\beta_p^A$ . The  $pK_a$  values of protonated morpholine and pyrrolidine are 8.36 and 11.27, respectively.<sup>9</sup> The  $\beta^L$  value is  $-0.83$  which may be compared with a  $\beta_{1g}^L$  of  $-0.52$  for the effect of endocyclic nitrogen basicity on endocyclic C–N bond fission. The  $\beta_p^A$  for the effect of exocyclic nitrogen basicity on ring opening and  $\beta$ -amino amide formation is  $-0.71$ , which is much more negative than the  $\beta_p^L$  of  $-0.07$  observed for  $\beta$ -lactam formation.

The interpretation of the  $\beta$  values for leaving groups is complicated because the increasing electron density developing in nitrogen resulting from C–N bond fission is opposed by the generation of positive charge resulting from protonation (8) and (9). These effects are discussed in the next section.

There is a marked difference between the effect of basicity of the nitrogen which becomes the product amide or  $\beta$ -lactam, *i.e.* the  $\beta_p$  values. This could simply be the result of differences between arylamines, used as the probe for endocyclic nitrogen, compared with alkylamines, used as the probe for exocyclic nitrogen. However, this is not observed in other systems.<sup>3</sup> Given that there is a large amount of charge on the exocyclic nitrogen in the reactant amidinium salt a  $\beta_p^A$  of  $-0.71$  indicates that there is little charge on the exocyclic nitrogen in the transition state for  $\beta$ -amino amide formation (9). This is compatible with an early transition state for the breakdown of  $T^\circ$  to give a  $\beta$ -amino amide by opening the four-membered ring. A transition state for  $\beta$ -amino amide formation which resembles  $T^\circ$  is also

compatible with the  $\beta_{1g}^A$  of  $-0.52$ . The  $\beta_p^L$  of  $-0.07$  indicates a large amount of positive charge on the endocyclic nitrogen in the transition state for exocyclic C–N bond fission and  $\beta$ -lactam formation (4). This is compatible with a late transition state for the decomposition of  $T^\circ$  in which there is considerable bond formation and breakage such that a positive charge develops on the incipient  $\beta$ -lactam nitrogen due to resonance. This is also compatible with the  $\beta_{1g}^L$  of  $-0.83$ , suggesting significant exocyclic C–N bond fission, and the  $\alpha$  value of 0.59 suggesting significant proton transfer in the transition state (14).



*Structure-Reactivity Relationships and the Reaction Mechanism.*—Although the data is not as fully comprehensive as we would like, we have obtained the effect of changing both endo- and exo-cyclic nitrogen basicity on the Brønsted  $\alpha$ -values for the buffer-catalysed formation of both  $\beta$ -lactam and  $\beta$ -amino amide (Table 3). In Table 5 is shown the effect of changing the acidity of the buffer catalyst on the  $\beta_{1g}$  and  $\beta_p$  values for both exocyclic and endocyclic C–N bond fission.

From Table 3 it can be seen that as the basicity of the leaving group decreases (a better leaving group in the classic sense of a more stable amine anion) the rate of the reaction becomes less dependent upon the acidity of the proton donor. The  $\alpha$  value decreases from 0.40 to 0.17 on changing from a phenyl- to a 4-nitrophenyl-amine leaving group (5) (X = H *versus* X = NO<sub>2</sub>), for  $\beta$ -amino amide formation. Similarly, for  $\beta$ -lactam formation, the  $\alpha$  value decreases from 0.59 to 0.36 as the leaving-group amine changes from pyrrolidine to the less basic morpholine [(5) *versus* (7)].

The opposite effect is observed if the basicity is changed of the nitrogen which is not expelled from  $T^\circ$  and which becomes the product amide or  $\beta$ -lactam nitrogen (Table 3). The rate of  $\beta$ -lactam and  $\beta$ -amino amide formation becomes more dependent on the acidity of the proton donor as the remaining nitrogen is made less basic. For  $\beta$ -lactam formation,  $\alpha$  increases from 0.43 to 0.59 as electron-withdrawing substituents are attached to the incipient  $\beta$ -lactam nitrogen (5) (X = H *versus* X = NO<sub>2</sub>). The effect for amino amide formation is less marked but nonetheless in the same direction as  $\alpha$  increases from 0.17 to 0.25 as the amine of the incipient amide changes from pyrrolidine to the less electron-donating morpholine [(5) *versus* (7)].

The effect of changing the acidity of the buffer catalyst on the Brønsted  $\beta_{1g}$  and  $\beta_p$  values is not large (Table 5) except for the most acidic buffer, phosphate (Table 5). The large differences observed for phosphate may be due to the fact that the mechanism changes from hydroxide ion to water addition to the amidinium salt at low pH (*vide supra*). However, there is a tendency for the  $\beta_{1g}$  values for both  $\beta$ -amino amide and  $\beta$ -lactam formation to increase and become less negative as the acidity of the proton donor increases.

The change in  $\alpha$  values with leaving group basicity (Table 3) indicates that in the transition state (15), the proton is transferred to a lesser extent to the departing nitrogen in the case of the more *weakly basic* amine. This is in the opposite direction to that observed in the general-acid-catalysed breakdown of the anionic tetrahedral intermediate (16) formed during the lactonisation of a hydroxyamide.<sup>10</sup> Although the present behaviour is also the opposite of that predicted by the classic Polanyi–Bell–Leffer–Hammond postulates<sup>11</sup> in terms of ease of protonation it is that predicted from a consideration

**Table 5.** Brønsted exponents  $\beta_{1g}$  and  $\beta_p$  for  $\beta$ -amino amide (A; endocyclic fission) and  $\beta$ -lactam (L; exocyclic fission) formation for the hydrolysis of azetidyl amidinium salts.

Buffer catalyst	pK <sub>a</sub>	Brønsted exponent			
		$\beta_{1g}^A$	$\beta_{1g}^L$	$\beta_p^L$	$\beta_p^A$
Water	15.74	-0.52	-0.83	-0.07	-0.71
Trifluoroethanol	12.43	-0.58	-0.89	+0.04	-0.51
Quinuclidine	11.55	-0.48	—	—	-0.43
1,1,1,3,3,3-Hexafluoro- propan-2-ol	9.30	-0.50	-0.75	-0.08	-0.56
Phosphate	6.80	-0.21	-0.42	—	—



of a Jencks–More O’Ferrall diagram<sup>12–14</sup> for a concerted coupled breakdown of the tetrahedral intermediate  $T^\circ$ . Figures 5 and 6 show Jencks–More O’Ferrall diagrams for  $\beta$ -amino amide and  $\beta$ -lactam formation with substituent changes in the endocyclic nitrogen whereas Figures 7 and 8 do the same for changes in basicity of the exocyclic nitrogen.

Figure 5 illustrates the two processes of carbon–endocyclic nitrogen bond fission and protonation of endocyclic nitrogen that occur when the tetrahedral intermediate  $T^\circ$  is converted into the  $\beta$ -amino amide. For simplicity, the conjugate acid of the amide is written as the apparent product along the top edge. This should not be taken to imply that we believe that this actually occurs. Deprotonation of the hydroxy group of  $T^\circ$  may occur simultaneously with C–N bond fission and protonation. Movement along the left- and right-hand edges represents carbon–nitrogen bond fission with no proton transfer and movement along the top and bottom edges represents proton transfer with no carbon–nitrogen bond fission. The amount of ‘coupling’ between atomic motions, carbon–nitrogen bond fission and proton transfer, indicates the amount of ‘concertedness’ of the reaction. For a diagonal reaction co-ordinate as shown in Figure 5 where the Brønsted  $\alpha$  coefficient for proton transfer is shown along the horizontal co-ordinate and the amount of C–endocyclic N bond cleavage along the vertical co-ordinate. Charge development on the leaving group as measured by  $\beta_{1g}$  increases along a diagonal co-ordinate and reflects the fact that  $\beta_{1g}$  may increase either because of an increased amount of protonation or because of less C–N bond fission in the transition state, *i.e.*  $\beta_{1g}$  increases along the horizontal axis left to right and increases along the vertical axis, top to bottom.

A decrease in the basicity of the aniline upon addition of an electron-withdrawing substituent will destabilise the tetrahedral intermediate  $T_A^+$ , but stabilise the aniline anion,  $ArN^-$ , and so lower the energy of the upper left relative to the lower right of the diagram. For a diagonal reaction co-ordinate (Figure 5) the position of the transition state will tend to slide ‘downhill’ towards the upper left corner (perpendicular to the reaction co-ordinate). The horizontal axis of the diagram describes the amount of proton transfer, as measured by the Brønsted  $\alpha$  value, so that this shift represents a decrease in  $\alpha$  which is observed (Table 3).

An increase in the acidity of the catalysing acid raises the energy of the left-hand edge of the diagram relative to the right-

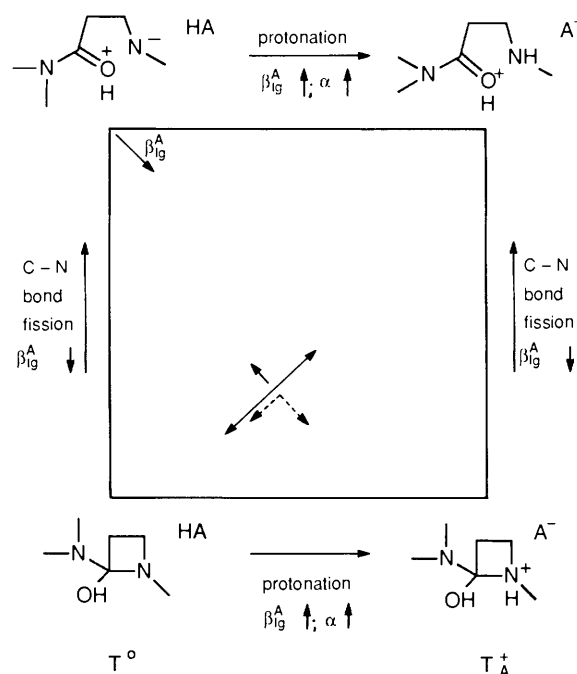


**Figure 5.** More O’Ferrall–Jencks diagram based on structure–activity relationships for the general-acid-catalysed breakdown of the tetrahedral intermediate  $T^\circ$  to a  $\beta$ -amino amide (Scheme 2). The vertical and horizontal axes are defined by the amount of C–N bond fission and the Brønsted  $\alpha$  coefficient, respectively. The Brønsted  $\beta_{1g}^A$  for substituents attached to the endocyclic nitrogen is defined by the diagonal arrow (top left to bottom right). The diagonal double-headed arrow (bottom left to top right) represents the reaction co-ordinate from which the solid arrow indicates the expected change in  $\alpha$  upon the addition of electron-withdrawing substituents to the endocyclic amine leaving group and the dashed arrow the expected change in  $\beta_{1g}^A$  as the proton donor HA is made a stronger acid.

hand edge. For a diagonal reaction co-ordinate (Figure 5) the transition state will then tend to slide downhill towards the bottom right, perpendicular to the reaction co-ordinate, and move uphill towards the bottom left, parallel to the reaction co-ordinate (‘a Hammond effect’). The  $\beta_{1g}^A$  value may increase as a result of a motion perpendicular to the diagonal reaction co-ordinate because of more proton transfer and less C–N bond fission. A motion parallel to the reaction co-ordinate may either increase  $\beta_{1g}^A$  because of reduced C–N bond fission or, decrease  $\beta_{1g}^A$  because of less proton transfer in the transition state. The observed effect is that there is little change in  $\beta_{1g}^A$  with increasing acidity of the catalyst other than perhaps a slight increase *i.e.* less negative (Table 5). The observations are compatible with a diagonal reaction co-ordinate or one with a vertical component. It appears that C–N bond fission and proton transfer are coupled for opening the four-membered ring.

In Figure 6 is shown the Jencks–More O’Ferrall diagram for  $\beta$ -lactam formation for a diagonal reaction co-ordinate. The Brønsted  $\alpha$  coefficient for proton transfer is again shown along the horizontal co-ordinate and the amount of C–N bond cleavage and charge development on the  $\beta$ -lactam nitrogen as measured by  $\beta_p^L$  is shown along the vertical co-ordinate. There is no change in  $\beta_p^L$  moving from left to right since the effect of the degree of proton transfer to the departing nitrogen has little effect on this remaining nitrogen.

A decrease in the basicity of the endocyclic nitrogen upon addition of an electron-withdrawing substituent will stabilise  $T_L^+$  relative to the  $\beta$ -lactam. Perpendicular to the reaction co-ordinate, this will lower the energy of the lower right- relative to the upper left-hand of the diagram, resulting in a shift of the



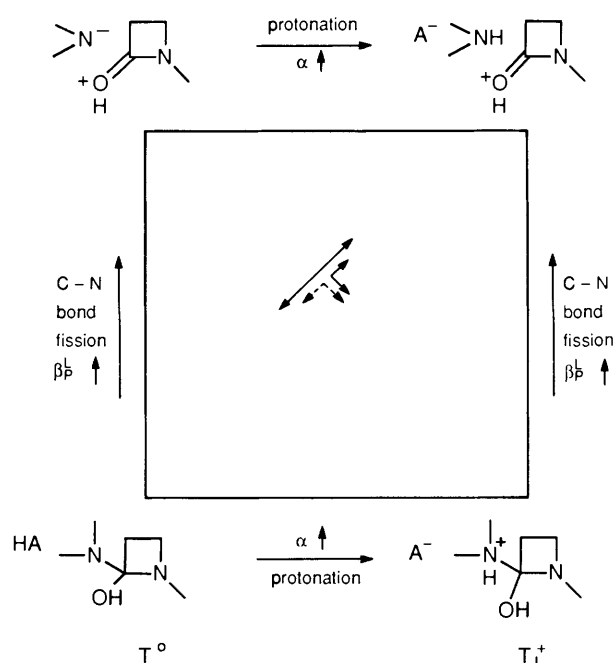


**Figure 6.** More O'Ferrall-Jencks diagram based on structure-activity relationships for the general-acid-catalysed breakdown of the tetrahedral intermediate  $T^\circ$  to a  $\beta$ -lactam (Scheme 2). The horizontal axis is defined by the Brønsted coefficient  $\alpha$ . The Brønsted  $\beta_p^L$  for the effect of substituents attached to the endocyclic nitrogen is defined by the vertical axis. The diagonal double-headed arrow (bottom left to top right) represents the reaction co-ordinate from which the solid arrows indicate the expected change in  $\alpha$  upon the addition of electron-withdrawing substituents to the endocyclic nitrogen and the expected change in  $\beta_p^L$  as the proton donor HA is made a stronger acid.

transition state downhill towards the lower right-hand corner causing more proton transfer to the exocyclic nitrogen and so consequently an increase in  $\alpha$  which is observed (an 'anti-Hammond effect'). Parallel to the reaction co-ordinate electron-withdrawing substituents will stabilise the lower left of the diagram, resulting in an uphill shift of the transition state towards the upper right. This may result in more proton transfer and an increase in  $\alpha$ . Both parallel and antiparallel effects are therefore compatible with the observations (Table 3).

An increase in the acidity of the catalyst raises the energy of the left-hand edge of the diagram relative to the right-hand edge (Figure 6). For a diagonal reaction co-ordinate, the transition state will then move downhill towards the bottom right for perpendicular motion (an 'anti-Hammond effect') and move uphill towards the bottom left for parallel motion (a 'Hammond effect'). Both motions predict therefore a decrease in  $\beta_p^L$  as the  $pK_a$  of the acid catalyst decreases. However, the observed effect on  $\beta_p^L$  with changing acidity of the proton donor is minimal (Table 5).

In Figure 7 is shown the diagram for  $\beta$ -lactam formation where charge development on the exocyclic nitrogen is measured by  $\beta_{1g}^L$  which increases diagonally as a result of more protonation or less C-N bond fission in the transition state.

A decrease in the basicity of the exocyclic amine nitrogen will destabilise the tetrahedral intermediate  $T_L^+$  but stabilise the amine anion, so lowering the energy of the top left relative to the bottom right of the diagram. For a diagonal reaction co-ordinate the antiparallel effect will move the transition state towards the upper left-hand corner so that  $\alpha$  will decrease, which is observed (Table 3).

An increase in acidity of the catalyst raises the energy of the left-hand side relative to the right-hand side (Figure 7). Hence  $\beta_{1g}^L$  may increase by an antiparallel effect or either increase or

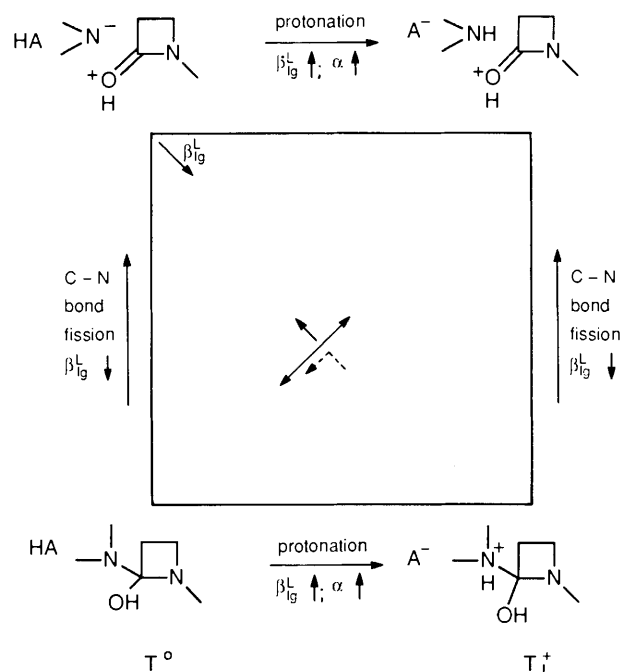


**Figure 7.** More O'Ferrall-Jencks diagram based on structure-activity relationships for the general-acid-catalysed breakdown of the tetrahedral intermediate  $T^\circ$  to a  $\beta$ -lactam (Scheme 2). The vertical and horizontal axes are defined by the amount of C-N bond fission and the Brønsted  $\alpha$  coefficient, respectively. The Brønsted  $\beta_{1g}^L$  for substituents attached to the exocyclic nitrogen is defined by the diagonal arrow (top left to bottom right). The diagonal double-headed arrow (bottom left to top right) represents the reaction co-ordinate from which the solid arrow indicates the expected change in  $\alpha$  upon addition of electron-withdrawing substituents to the exocyclic amine leaving group and the dashed arrow the expected change in  $\beta_{1g}^L$  as the proton donor HA is made a stronger acid.

decrease by a parallel effect to a diagonal reaction co-ordinate. The observed effect is that there is a slight increase in  $\beta_{1g}^L$ , i.e.,  $\beta_{1g}^L$  becomes less negative as the  $pK_a$  of the proton donor decreases (Table 5).

Finally, in Figure 8, is shown the effect of substituent changes in the exocyclic nitrogen on  $\beta$ -amino amide formation. Charge development on the nitrogen is indicated by  $\beta_p^A$  which increases along the vertical co-ordinate but does not change from the left to the right side i.e. it is dependent on C-N fission and not the degree of proton transfer to the departing endocyclic amine nitrogen. Making the endocyclic nitrogen less electron donating and less basic will move the transition state for a diagonal reaction co-ordinate towards the top right by a parallel effect and towards the bottom right by an antiparallel effect and so increase  $\alpha$ , which is the observed effect (Table 3).

An increase in acidity of the catalyst will move the transition state for a diagonal reaction co-ordinate towards the bottom edge and so decrease  $\beta_p^A$ . However, there is little or no change in the observed  $\beta_p^A$  as the  $pK_a$  of the buffer decreases (Table 5).

There are several cases where the effect of substituents placed in different parts of the reactants apparently do not give the same index of reaction progress in the transition state.<sup>15</sup> This is usually interpreted in terms of an imbalance between the apparent changes in the effective charges developed in the transition state as 'felt' by the substituents.<sup>15</sup> A well-documented case is the apparent imbalance as a result of resonance stabilisation present in the reactant or product being only partially present in the transition state because of concurrent solvation or hybridisation changes required to allow resonance interaction to occur.<sup>16</sup> Solvation effects can modify

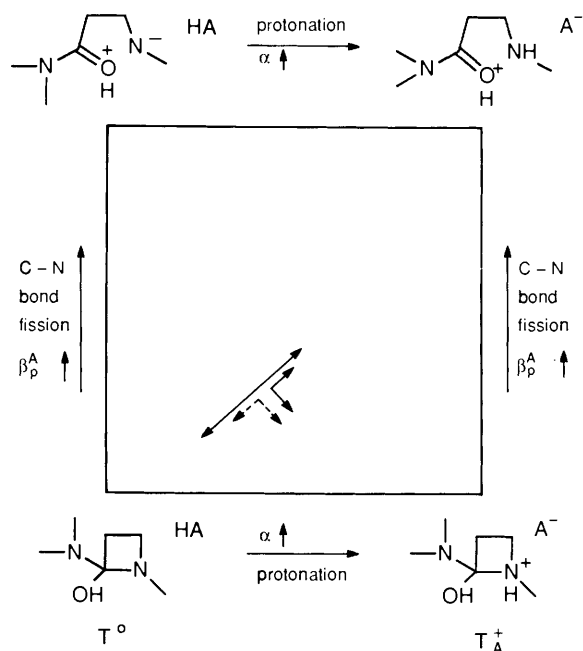


**Figure 8.** More O'Ferrall-Jencks diagram based on structure-activity relationships for the general-acid-catalysed breakdown of the tetrahedral intermediate  $T^\ominus$  to a  $\beta$ -amino amide (Scheme 2). The horizontal axis is defined by the Brønsted coefficient  $\alpha$ . The Brønsted  $\beta_p^A$  for the effect of substituents attached to the exocyclic nitrogen is defined by the vertical axis. The diagonal double-headed arrow (bottom left to top right) represents the reaction co-ordinate from which the solid arrows indicate the expected change in  $\alpha$  upon the addition of electron-withdrawing substituents to the exocyclic nitrogen and the expected change in  $\beta_p^A$  as the proton donor HA is made a stronger acid.

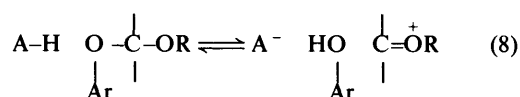
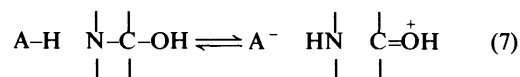
the interpretation of observed structure-reactivity relationships in terms of bond making and breaking.<sup>17,18</sup> This is the case when there are large differences in structure between the reactants/transition state and the reactants/products in the reference ionisation reaction. For example, the nitrogen lone pair in the reference ionisation reaction is hydrogen-bonded to water. This is presumably also the case in the tetrahedral intermediate  $T^\ominus$  provided it has a sufficiently long lifetime for solvation changes to occur. However, for this lone pair to assist expulsion of the leaving-group amine, desolvation must occur which is more difficult for more basic amines, giving rise to a negative  $\beta_p$  value.

Although the use of linear free-energy relationships to deduce transition-state structures has been questioned,<sup>19</sup> there is no doubt that, when used with care, they are meaningful and that substituent effects on the stability of transition states can be treated in a way similar to their effects on equilibria.<sup>17,20</sup>

The low value of  $\alpha$  (ca. 0.2) for the buffer-catalysed formation of the  $\beta$ -amino amide from the hydrolysis of (**5**; X = NO<sub>2</sub>) indicates that only a small amount of proton transfer occurs in the transition state and may indicate hydrogen-bond stabilisation of the transition state, rather than a proton in 'flight'.<sup>21,22</sup>

Finally, it is interesting to compare our observations with other reactions involving the general-acid-catalysed expulsion of leaving groups. Comparison has already been made with the breakdown of the anionic tetrahedral intermediate (**16**) for which changes in structure-activity relationships are the opposite<sup>10</sup> of those observed for the hydrolysis of the azetidiny amidinium salts. The general-acid-catalysed breakdown of  $T^\ominus$  [Scheme 2 and equation (7)] is analogous to that for the hydrolysis of substituted phenyl acetals [equation (8)] which

also shows a decrease in  $\alpha$  with a decrease in the  $pK_a$  of the leaving phenol.<sup>23</sup> Similar observations have been made for the general-acid-catalysed formation of semicarbazones.<sup>24</sup> The carbonium ion formed in acetal hydrolysis, equation (8) is less stable than the protonated amide which may be the initial product of breakdown of  $T^\ominus$  [equation (7)]. The acetal oxygen leaving group is also much less basic than the amine nitrogen, so it is not surprising that acetal hydrolysis appears to be accompanied by significant carbon-oxygen bond fission in the transition state.<sup>23</sup>



### Acknowledgements

We are grateful to the UK SERC for the award of a research studentship to P.W.

### References

- M. I. Page, P. Webster, and L. Ghosez, *J. Chem. Soc., Perkin Trans. 2*, 1990, preceding paper.
- C. Hoornaert, A. M. Hesbain-Frisque, and L. Ghosez, *Angew. Chem., Int. Ed. Engl.*, 1975, **14**, 569; J. Marchant-Brynaert, M. Portuguez, I. Huber, and L. Ghosez, *J. Chem. Soc., Chem. Commun.* 1983, 818; M. De Poortere, J. Marchand-Brynaert, and L. Ghosez, *Angew. Chem., Int. Ed. Engl.* 1974, **13**, 267.
- P. Proctor, N. P. Gensmantel, and M. I. Page, *J. Chem. Soc., Perkin Trans. 2*, 1982, 1185.
- M. I. Page, *Chem. Soc. Rev.*, 1973, 295; C. J. M. Stirling, *Tetrahedron*, 1985, **41**, 1613; M. A. Casadei, A. di Martino, C. Galli, and L. Mandolini, *Gazz. Chim. Ital.*, 1986, **116**, 659.
- Y. N. Lee and G. L. Schmir, *J. Am. Chem. Soc.*, 1979, **101**, 3026.
- A. Williams, *Acc. Chem. Res.*, 1984, **17**, 425; W. P. Jencks, *Cold Spring Harbour Symp. Quant. Biol.*, 1971, **36**, 1.
- M. I. Page, *Adv. Phys. Org. Chem.*, 1987, **23**, 165.
- E. Grunwald, K. C. Chang, P. L. Skipper, and V. K. Anderson, *J. Phys. Chem.*, 1976, **80**, 1425.
- W. P. Jencks and J. Regenstein, 'Handbook of Biochemistry,' J-150, 1968.
- J. J. Morris and M. I. Page, *J. Chem. Soc., Perkin Trans. 2*, 1980, 685.
- M. G. Evans and M. Polanyi, *Trans. Faraday Soc.*, 1938, **34**, 11; R. P. Bell 'The Proton in Chemistry,' Cornell University Press, Ithaca, 1973, 2nd edn., p. 206; J. E. Leffler, *Science*, 1953, **117**, 340; G. S. Hammond, *J. Am. Chem. Soc.*, 1955, **77**, 334.
- R. A. More O'Ferrall, *J. Chem. Soc. B.*, 1970, 274.
- D. A. Jencks and W. P. Jencks, *J. Am. Chem. Soc.*, 1977, **99**, 7948.
- E. D. Hughes, C. K. Ingold, and V. G. Shapiro, *J. Chem. Soc.*, 1936, 225; J. F. Bunnett, *Angew. Chem., Int. Ed. Engl.*, 1962, **1**, 225.
- J. M. Sayer and W. P. Jencks, *J. Am. Chem. Soc.*, 1977, **99**, 464; L. H. Funderburk and W. P. Jencks, *ibid.*, 1978, **100**, 6708; C. F. Bernasconi, *Tetrahedron*, 1985, **41**, 3219.
- F. G. Bordwell and W. J. Boyle, Jr., *J. Am. Chem. Soc.*, 1972, **94**, 3907; A. J. Kresge, *Can. J. Chem.* 1974, **52**, 1897; J. P. Richard, M. E. Rothenberg, and W. P. Jencks, *J. Am. Chem. Soc.*, 1984, **106**, 1361.
- W. P. Jencks, *Chem. Rev.*, 1985, **85**, 511; W. P. Jencks, *Bull. Soc. Chim. Fr.*, 1988, 218.
- W. P. Jencks, M. T. Haber, D. Herschlag, and K. L. Nazaretian, *J. Am. Chem. Soc.*, 1982, **104**, 7045; D. J. Hupe and E. R. Pohl, *ibid.*, 1984, **106**, 5634; D. J. Hupe and W. P. Jencks, *ibid.*, 1977, **99**, 451; C. J. Murray and W. P. Jencks, *ibid.*, 1988, **110**, 7561; J. P. Richard, *J. Chem. Soc., Chem. Commun.*, 1987, 1268.
- A. Pross, *J. Org. Chem.*, 1984, **49**, 1811; S. S. Shaik, *Prog. Phys. Org. Chem.*, 1985, **15**, 197; G. Lamaty and C. Menut, *Pure Appl. Chem.*,

- 1982, **54**, 1837; J. P. Guthrie, *J. Am. Chem. Soc.*, 1980, **102**, 5286; S. Formosinho, *J. Chem. Soc., Perkin Trans. 2*, 1987, **61**.
- 20 E. Buncl, I. H. Um, and S. Hoz, *J. Am. Chem. Soc.*, 1989, **111**, 971.
- 21 M. M. Cox and W. P. Jencks, *J. Am. Chem. Soc.*, 1981, **103**, 572; H. F. Gilbert and W. P. Jencks, *ibid.*, 1977, **99**, 7931.
- 22 L. D. Kershner and R. L. Schowen, *J. Am. Chem. Soc.*, 1971, **93**, 2014.
- 23 B. Capon and K. Nimmo, *J. Chem. Soc., Perkin Trans. 2.*, 1975, 1113.
- 24 L. H. Funderburk and W. P. Jencks, *J. Am. Chem. Soc.*, 1978, **100**, 6708.

*Paper 9/04764F*

*Received 6th November 1989*

*Accepted 24th January 1990*